Finlines in Rectangular and Circular Waveguide Housings Including Substrate Mounting and Bending Effects—Finite Element Analysis

ESWARAPPA, STUDENT MEMBER, IEEE, GEORGE I. COSTACHE, SENIOR MEMBER, IEEE, AND WOLFGANG J. R. HOEFER, SENIOR MEMBER, IEEE

Abstract—**The finite element method is applied for deriving the dispersion characteristics and field components of dominant and higher order modes in finlines. The method is accurate and covers the metallization thickness, substrate mounting grooves, bending of the substrate, and arbitrary cross sections. Results for structures already obtained with other methods have been found to agree well with available data. As a new contribution, the effect of substrate bending on the propagation constant is studied. Also, the dispersion characteristics for the dominant and higher order modes for bilateral finlines in circular waveguide housing are calculated for the first time. The field plots for all the modes are also given.**

I. Introduction

FINLINES are of increasing importance for millimeter-wave integrated circuits because of their wide bandwidth for single-mode operation, low dispersion in the frequency range of interest, moderate attenuation, and compatibility with solid-state devices. Various methods have been applied to calculate the cutoff frequencies, dispersion characteristics, and characteristic impedances of finlines in rectangular waveguide enclosures [1]–[5]. Only two papers [6], [7] have so far been published which deal with the computation of finline losses. However, the results of these papers disagree by as much as 100 percent. Most of these methods can only handle structures of regular cross-sectional geometry.

The purpose of this study was to develop a very general finite element method of analysis which can handle arbitrary cross-sectional geometries, including mounting effects, imperfections such as the bending of the substrate (which can occur due to improper mounting of soft substrate), and the cross-sectional profile of the metallization edges. The last effect is of particular importance in the computation of losses and power-handling capacities. In addition, the finite element analysis allows the study of previously neglected configurations such as finlines in circular waveguide enclosures. It is interesting to note that a similar structure was first proposed by Robertson [15] under the name of finline. The paper presents the dispersion characteristics of the fundamental and higher order modes of such a structure.

Manuscript received January 25, 1988; revised July 20, 1988. This work was supported by the Canadian Commonwealth Scholarship and Fellowship Administration and by the Natural Science and Engineering Research Council of Canada.

The authors are with the Laboratory for Electromagnetics and Microwaves, Department of Electrical Engineering, University of Ottawa, Ottawa, Ont., Canada K1N 6N5.

IEEE Log Number 8824995.

II. Theory

The finite element method is based on a variational principle. Several vectorial variational formulations have been proposed. These can be classified into the following four types:

i) variational expressions which are formulated in terms of the longitudinal components of the electric field (E_z) and the magnetic field (H_z) [8];
ii) variational expressions employing all three components of the electric field [9];
iii) variational expressions employing all three components of the magnetic field [10], [11];
iv) variational expressions employing the transverse electric and magnetic field components [12].

The first type of variational formulation is chosen for our purpose because of its simplicity and the small matrix size of the eigenvalue problem.

Consider a waveguide of arbitrary shape uniform in the z direction which consists of isotropic, lossless dielectric media. Assume that the cross section can be divided into several subregions over which the relative permittivity is constant. Further, assume propagation along the z axis of the form $\exp[j(\omega t - \beta z)]$ with longitudinal field components H_z and E_z. In a typical subregion (say the pth), E_z and H_z satisfy the Helmholtz equations:

$$\left(\nabla_t^2 + K_p^2\right)\begin{bmatrix} E_z^{(p)} \\ H_z^{(p)} \end{bmatrix} = 0. \tag{1}$$

where ∇_t^2 is the transverse Laplacian operator, and K_p^2 is given by

$$K_p^2 = (\omega/c)^2(\epsilon_p/\epsilon_0) - \beta^2 \tag{2}$$

with ϵ_p as the dielectric permittivity. Continuity of the tangential electric and magnetic fields along the common interface between two contiguous regions (say the pth and

0018-9480/89/0200-0299$01.00 ©1989 IEEE

qth) requires that

$$E_z^{(p)} = E_z^{(q)}$$

$$H_z^{(p)} = H_z^{(q)}$$

$$\tau_p\left[\gamma\left(\frac{\epsilon_0}{\mu_0}\right)^{1/2}\frac{\partial E_z^{(p)}}{\partial s} - \frac{\partial H_z^{(p)}}{\partial n}\right] = \tau_q\left[\gamma\left(\frac{\epsilon_0}{\mu_0}\right)^{1/2}\frac{\partial E_z^{(q)}}{\partial s} - \frac{\partial H_z^{(q)}}{\partial n}\right]$$

$$\tau_p\left[\frac{\epsilon_p}{\epsilon_0\gamma}\left(\frac{\epsilon_0}{\mu_0}\right)^{1/2}\frac{\partial E_z^{(p)}}{\partial n} + \frac{\partial H_z^{(p)}}{\partial s}\right] = \tau_q\left[\frac{\epsilon_q}{\epsilon_0\gamma}\left(\frac{\epsilon_0}{\mu_0}\right)^{1/2}\frac{\partial E_z^{(q)}}{\partial n} + \frac{\partial H_z^{(q)}}{\partial s}\right] \quad (3)$$

where s and n refer to the tangential and normal directions, respectively, with $n \times s = e_z$ defining the unit normal along the z direction. The quantities τ_i and γ are given by

$$\tau_i = (\gamma^2 - 1)/(\gamma^2 - \epsilon_i/\epsilon_0)$$

$$\gamma = (\beta c)/\omega. \quad (4)$$

The variational principle

$$\delta I = 0 \quad (5)$$

where

$$I = \sum_{p=1} I_p$$

$$= \sum_{p=1}\int\int\left(\tau_p|\nabla H_z^{(p)}|^2 + \gamma^2\tau_p\frac{\epsilon_p}{\epsilon_0}\left|\frac{1}{\gamma}\left(\frac{\epsilon_0}{\mu_0}\right)^{1/2}\nabla E_z^{(p)}\right|^2 + 2\tau_p\hat{e}_z\gamma^2\cdot\left[\frac{1}{\gamma}\left(\frac{\epsilon_0}{\mu_0}\right)^{1/2}\nabla E_z^{(p)}\times\nabla H_z^{(p)}\right] - \left(\frac{\omega}{c}\right)^2(1-\gamma^2)\cdot\left\{\left[H_z^{(p)}\right]^2 + \gamma^2\frac{\epsilon_p}{\epsilon_0}\left[\frac{1}{\gamma}\left(\frac{\epsilon_0}{\mu_0}\right)^{1/2}E_z^{(p)}\right]^2\right\}\right)dx\,dy \quad (6)$$

yields as its Euler equations and natural boundary conditions the governing equations (1) and continuity conditions (3) for all regions constituting the waveguide cross section.

III. Discretization

The bases for generating the finite element algorithm are equation (5) with the functional (6). The initial step is the discretization of the waveguide cross section into a large number of subregions or elements in an arbitrary manner, provided that all the dielectric interfaces coincide with the element sides. Although a variety of different elements can be chosen, the triangular [13],]14] second-order elements are adopted in this study. The values of E_z and H_z at the element vertices or nodes will be considered as the primary dependent variables of the problem. In a triangle, the E_z and H_z fields are approximated by a linear combination of a complete set of interpolation polynomials $\{\alpha_i,\ i = 1,2,3,\cdots,n\}$, each of degree N:

$$E_z = \sum_{i=1}^{n} E_{zi}\alpha_i(\zeta_1,\zeta_2,\zeta_3)$$

$$H_z = \sum_{i=1}^{n} H_{zi}\alpha_i(\zeta_1,\zeta_2,\zeta_3) \quad (7)$$

where

$$n = \frac{(N+1)(N+2)}{2}.$$

The coefficients E_{zi} and H_{zi} represent the values of E_z and H_z, respectively, at the interpolation nodes; ζ_1, ζ_2, and ζ_3 are triangle coordinates. After substituting the above expressions for E_z and H_z into (6), I_p can be written in matrix form as

$$I_p = [\theta_p]^T[A_p][\theta_p] - \Gamma[\theta_p]^T[B_p][\theta_p] \quad (8)$$

where Γ is the eigenvalue parameter defined by

$$\Gamma = \left(\frac{\omega}{c}\right)^2(1-\gamma^2) \quad (9)$$

and $[\theta_p]$ is the assembled array of nodal E_z and H_z values, given by

$$[\theta_p]^T = [E_{z1}, E_{z2},\cdots, E_{zn}, H_{z1}, H_{z2},\cdots, H_{zn}]. \quad (10)$$

The matrices $[A_p]$ and $[B_p]$ are given by

$$[A_p] = \tau_p\begin{pmatrix}\frac{\epsilon_p}{\epsilon_0}\gamma^2 S & 2\gamma^2 U\\ -2\gamma^2 U & S\end{pmatrix} \quad (11)$$

$$[B_p] = \begin{pmatrix}\frac{\epsilon_p}{\epsilon_0}\gamma^2 T & 0\\ 0 & T\end{pmatrix}. \quad (12)$$

Matrices S, T, and U are square matrices of order n, the first two being derived in [13] and the last one in [14]. All three matrices are independent of the properties of the medium. These base matrices are successively applied to the total number of triangles of a given structure to obtain the final matrices. Thus summing the contributions I_p of all the triangles yields the following equation for I:

$$I = [\theta]^T[A][\theta] - \Gamma[\theta]^T[B][\theta] \quad (13)$$

where $[\theta]$ is an ordered array of the longitudinal electromagnetic nodal variables, $[A]$ is a large sparse indefinite symmetric matrix, and $[B]$ is a large sparse positive-definite symmetric matrix. Variation of (13) with respect to the nodal variables leads to the following algebraic eigenvalue problem:

$$[A][\theta] = \Gamma[B][\theta]. \quad (14)$$

The parameter γ is present in the matrices $[A]$ and $[B]$. For a given value of γ, the above generalized eigenvalue equation is solved for the frequency and the longitudinal

electromagnetic nodal variables. All transverse field components can be derived from the longitudinal field values by the equations

$$E_x^{(p)} = \frac{j\omega\mu_0}{K_p^2}\left[\frac{\partial H_z^{(p)}}{\partial y} + \left(\frac{\epsilon_0}{\mu_0}\right)^{1/2}\gamma\frac{\partial E_z^{(p)}}{\partial x}\right]$$

$$E_y^{(p)} = \frac{j\omega\mu_0}{K_p^2}\left[\frac{-\partial H_z^{(p)}}{\partial x} + \left(\frac{\epsilon_0}{\mu_0}\right)^{1/2}\gamma\frac{\partial E_z^{(p)}}{\partial y}\right]$$

$$H_x^{(p)} = \frac{j\omega\epsilon_0}{K_p^2}\left[-\frac{\epsilon_p}{\epsilon_0}\frac{\partial E_z^{(p)}}{\partial y} + \left(\frac{\mu_0}{\epsilon_0}\right)^{1/2}\gamma\frac{\partial H_z^{(p)}}{\partial x}\right]$$

$$H_y^{(p)} = \frac{j\omega\epsilon_0}{K_p^2}\left[\frac{\epsilon_p}{\epsilon_0}\frac{\partial E_z^{(p)}}{\partial x} + \left(\frac{\mu_0}{\epsilon_0}\right)^{1/2}\gamma\frac{\partial H_z^{(p)}}{\partial y}\right]. \quad (15)$$

It is possible to use the symmetry conditions to reduce the number of elements by imposing the following boundary conditions on the axes:

$E_z = 0$ at the nodes on the electric wall;
$H_z = 0$ at the nodes on the magnetic wall.

The propagation constant γ, which is a variational quantity, is obtained much more accurately than the associated field solution. Therefore, good accuracy of the loss and impedance calculations demands a larger number of elements than would be required for obtaining only γ with similar accuracy. Equation (14) usually has a number of spurious solutions, especially for $\gamma > 1$. These solutions do not correspond to a physical mode of propagation and can be eliminated by inspection of their field plots and secondary parameters such as transmitted power and attenuation constants, which differ by orders of magnitude from those obtained for regular solutions.

IV. Conductor and Dielectric Losses

The perturbational approach is employed to solve for the attenuation constants due to dielectric and conductor losses:

$$\alpha_d = \frac{P_d}{2P_{\text{av}}} \qquad \alpha_c = \frac{P_c}{2P_{\text{av}}} \quad (16)$$

where P_{av} is the time-averaged power flow along the line, and P_d and P_c are the time-averaged powers dissipated in the dielectric and conductors, respectively.

Dielectric losses are calculated using the formula

$$P_d = \omega\epsilon\tan\delta\int\int_{S_{\text{diel}}}|E_0|^2\,dS \quad (17)$$

where the loss tangent $\tan\delta$ is assumed to be very small so that the perturbed fields can be approximated by the fields for the lossless condition E_0, H_0; S_{diel} is the area of the cross section covered by the dielectric; and $\omega = 2\pi f$ is the angular frequency.

For any generalized structure, (17) can be expressed in matrix form as follows:

$$P_d = \omega\sum_{i=1}^{\text{NOTRD}}\epsilon_i\tan\delta_i\left(\left[\theta_{1E}^i\right]^T[T]\left[\theta_{1E}^i\right] + \left[\theta_{2E}^i\right]^T[T]\left[\theta_{2E}^i\right] + \left[\theta_{3E}^i\right]^T[T]\left[\theta_{3E}^i\right]\right) \quad (18)$$

where NOTRD is the number of elements in the dielectric region, the matrix T is as mentioned in the Section III, and $[\theta_{1E}^i]$, $[\theta_{2E}^i]$, and $[\theta_{3E}^i]$ are the electric field values at the nodes of triangle i:

$$\left[\theta_{1E}^i\right]^T = \left[E_{x1}^i, E_{x2}^i, \cdots, E_{xn}^i\right]$$
$$\left[\theta_{2E}^i\right]^T = \left[E_{y1}^i, E_{y2}^i, \cdots, E_{yn}^i\right]$$
$$\left[\theta_{3E}^i\right]^T = \left[E_{z1}^i, E_{z2}^i, \cdots, E_{zn}^i\right]. \quad (19)$$

Thus by knowing the electric nodal variables, the dielectric loss P_d can be computed.

The time-averaged power flow along the z direction can be written as

$$P_{\text{av}} = \int\int_S \text{Re}\left(\vec{E}_0 \times \vec{H}_0^*\right)\cdot\hat{a}_z\,ds \quad (20)$$

where S is the complete cross section. In terms of the transverse field components it is written as

$$P_{\text{av}} = \int\int_S \text{Re}\left(E_x H_y^* - E_y H_x^*\right)dx\,dy. \quad (21)$$

Using (15) and (7) and matrix equivalents of the various integrals given in [10], the above equation can be written in matrix form as follows:

$$P_{\text{av}} = \omega^2\mu_0\sum_{i=1}^{\text{NOTR}}\frac{\epsilon_i}{K_p^4}\left[\left\{\left(\epsilon_i + \gamma^2\right)\left[\theta_{3H}^i\right]^T[Z]\left[\theta_{3E}^i\right] + \sqrt{\frac{\mu_0}{\epsilon_0}}\gamma\left[\theta_{3H}^i\right]^T[D]\left[\theta_{3H}^i\right] + \epsilon_i\gamma\sqrt{\frac{\epsilon_0}{\mu_0}}\left[\theta_{3E}^i\right]^T[E]\left[\theta_{3E}^i\right]\right\} - \left\{\left(\epsilon_i + \gamma^2\right)\left[\theta_{3E}^i\right]^T[Z]\left[\theta_{3H}^i\right] - \sqrt{\frac{\mu_0}{\epsilon_0}}\gamma\left[\theta_{3H}^i\right]^T[E]\left[\theta_{3H}^i\right] - \epsilon_i\sqrt{\frac{\epsilon_0}{\mu_0}}\gamma\left[\theta_{3E}^i\right]^T[D]\left[\theta_{3E}^i\right]\right\}\right] \quad (22)$$

where

$$\left[\theta_{3E}^i\right]^T = \left[E_{z1}^i, E_{z2}^i, \cdots, E_{zn}^i\right]$$
$$\left[\theta_{3H}^i\right]^T = \left[H_{z1}^i, H_{z2}^i, \cdots, H_{zn}^i\right]. \quad (23)$$

The matrices $[Z]$, $[D]$, and $[E]$ are the same as the ones given in [10], and NOTR is the total number of elements. Thus by knowing the longitudinal field values, the time-averaged power flow can be computed.

The perturbational formula for calculating the conductor loss of a transmission line with a high-conductivity conductor is given by

$$P_c = R_s\int_C|\vec{H}_0|^2_{\text{tang}}\,dl \quad (24)$$

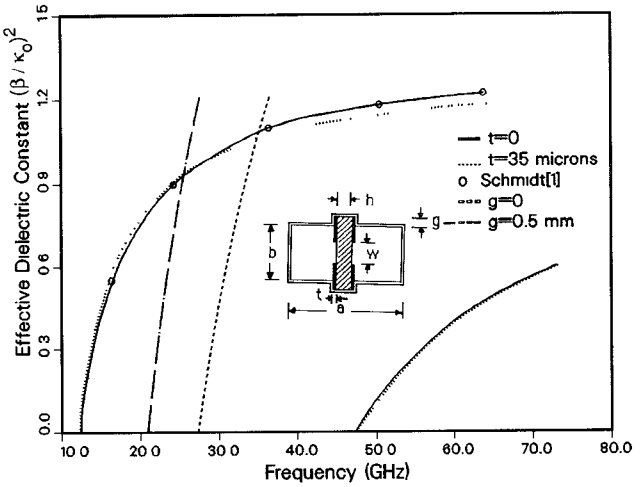

Fig. 1. Dispersion characteristics of a bilateral finline in rectangular waveguide housing (WR28). $\epsilon_r = 3.0$, $h = 0.125$ mm, $w = 0.5$ mm. ———— HE1 and HE7 modes for $t = 0$ and $g = 0$; · · · · · HE1 and HE7 modes for $t = 35$ μm and $g = 0$; ---- HE2 mode for $t = 0$ and $g = 0$; — · — HE2 mode for $t = 0$ and $g = 0.5$ mm.

where R_s is the surface resistance and $|\vec{H}_0|_{\text{tang}}$ is the magnitude of the tangential magnetic field at the conducting surfaces for the lossless case. Closed-form expressions have been derived to calculate the conductor loss (of the conducting surfaces lying on the x or the y axis) for second-order triangular elements. They are too lengthy to be given here. No numerical differentiation or integration is involved in the computation of losses.

V. Application to Finline Structures

On the basis of this finite element procedure, a computer program has been developed. With this program we have unprecedented flexibility since we can evaluate structures with arbitrary cross-sectional geometry. A very large number of elements are taken around the fin edges to account for the singularities. A CRAY X-MP/22 supercomputer has been used for computation.

A. Bilateral Finlines in Rectangular Waveguide Housing

In order to test the program, we have recalculated the characteristics of some standard finline structures, knowing well that for these cases other methods are more efficient. The dispersion characteristics of the dominant and higher order modes in a bilateral finline are shown in Fig. 1. The results for zero metallization thickness are in good agreement with data published by Schmidt [1] computed with the spectral-domain technique. For a metallization thickness $t = 35$ μm, the cutoff frequency of the dominant mode is slightly reduced because of increased capacitive loading of the guide. However, as the frequency increases, the crossover of the dispersion curves takes place. This may be attributed to the parallel-plate phenomenon because of the confinement of energy into the slot region. The dispersion characteristics of the higher mode remain unchanged. These results for finite metallization thickness conform to those given in [4]. The influence of the groove depth g on the propagation constant was also studied. It was found that the effect is negligible for the fundamental mode and the higher order mode HE7 (which are excited by a TE_{10} mode of the empty waveguide) as reported in [3] and [5]. However, the propagation characteristics of the second higher order mode HE2 are strongly affected. This behavior is illustrated in Fig. 1. The sensitivity of the second mode may be due to the fact that the fields for this mode are not concentrated around the fin edges and are rather confined between the two metal fins as in a parallel-plate capacitor. Hence the cutoff frequency for this mode is reduced with increasing groove depth.

TABLE I
Losses in Homogeneously Filled Waveguide

Finite Element Method Results			Analytical Results	
Frequency (GHz)	Conductor Loss (dB)	Dielectric Loss(dB)	Conductor Loss(dB)	Dielectric Loss(dB)
20 000	0 528	0 549	0 530	0 550
25 000	0 425	0 567	0 427	0 568
28.474	0 402	0 608	0 403	0 609
38 273	0 389	0 755	0 389	0.756

$a = 10$ mm, $b = 5$ mm, $\tan\delta = 2\times10^{-4}$, $\rho = 3\times10^{-8}$ $\Omega\cdot$m, $\epsilon_r = 1.0$.

TABLE II
Measured Losses For Bilateral Finlines in WR28 Waveguide Enclosures

Substrate	Thickness (microns)	Cu Metallization (microns)	Loss (dB/cm)		
			27 GHz	33 5 GHz	40GHz
Duroid 5880	127	17	0 06	0 06	0 06
Duroid 5880	254	17	0 07	0 07	0 13
Mylar	100	5	0 08	0 10	0 13
Kapton	75	34	0.13	0.14	0 20
Kapton	150	34	0.24	0 34	0 36

$w = 0.4$ mm [16].

In order to test the program for loss calculations, the conductor and dielectric losses of a homogeneously filled rectangular waveguide (WR28) have been computed at various frequencies. The dielectric had an ϵ_r of unity and a loss tangent of 2×10^{-8}. The resistivity of the walls was 3×10^{-8} $\Omega\cdot$m. Results are summarized in Table I. The results agree very well with the analytical values, thus supporting the accuracy of the presented numerical algorithm. The conductor and dielectric losses of a bilateral finline in rectangular waveguide enclosure (WR28) are given in Fig. 2(a). It is seen that as the gap width is reduced, the conductor loss increases exponentially. This can be explained by the fact that with small gap widths there is heavy concentration of fields near the gap. The dielectric losses are very small when compared to the

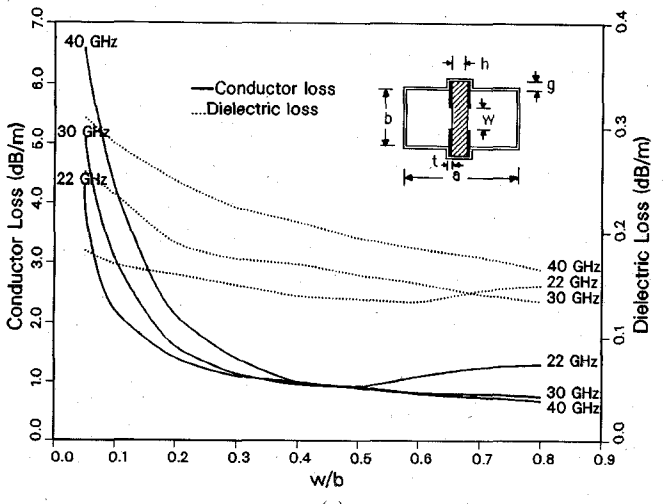

(a)

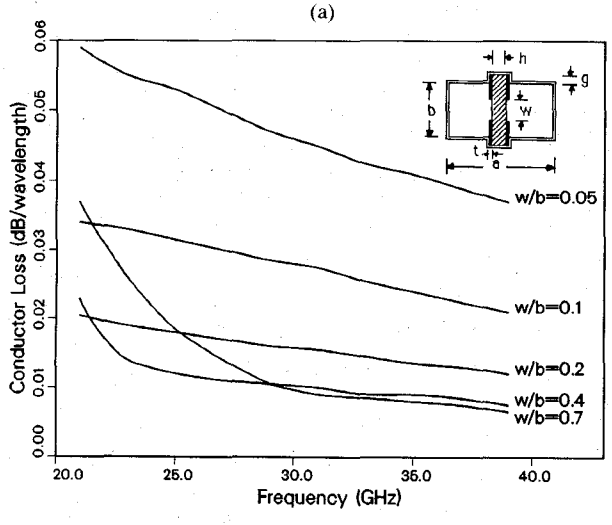

(b)

Fig. 2. Loss characteristics of a bilateral finline in rectangular waveguide housing (WR28). $h = 0.254$ mm, $\epsilon_r = 2.22$, $\tan\delta = 2\times10^{-4}$, $\rho = 3\times10^{-8}$ $\Omega\cdot$m. (a) Conductor and dielectric losses as a function of gap width (w). (b) Conductor loss per wavelength as a function of frequency.

conductor losses. The conductor loss per wavelength for various gap widths is plotted in Fig. 2(b) as a function of frequency. It appears that the losses obtained are between those of Mirshekar and Davies [6] and Olley and Rozzi [7] (assuming that the losses for bilateral and unilateral finlines are almost equal [6]). Independent measurement results are difficult to obtain. Bates and Coleman [16] have reported measured losses for bilateral finlines with slot widths of 400 μm. They are given in Table II. These measured losses are higher than our computed results. When we increased the elements around the fin edges (to account for the singularities), our results changed only by about 2 percent. Since in practice the measured losses are always higher than those predicted by theory because of such factors as surface roughness, irregularities in the structure, and anomalous skin effect, we believe that the theoretical losses we obtained are accurate.

Having tested our program by analyzing some well-known structures, we have applied it to compute certain novel structures.

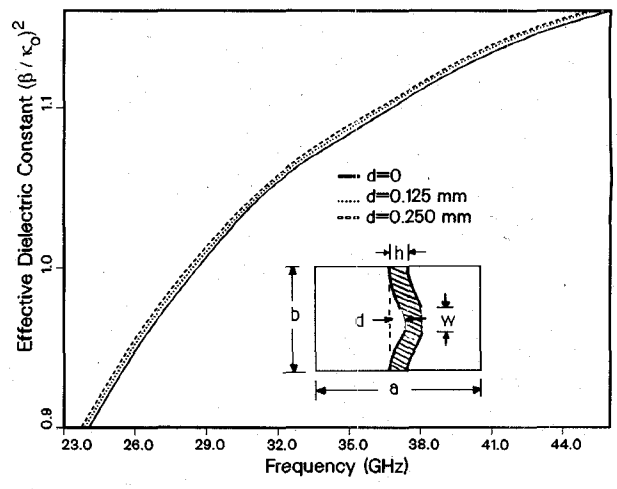

Fig. 3. Dispersion characteristics of a bilateral finline in rectangular waveguide (WR28) enclosure with bent substrate for different values of deflection d. $\epsilon_r = 3.0$, $h = 0.125$ mm, $w = 0.5$ mm.

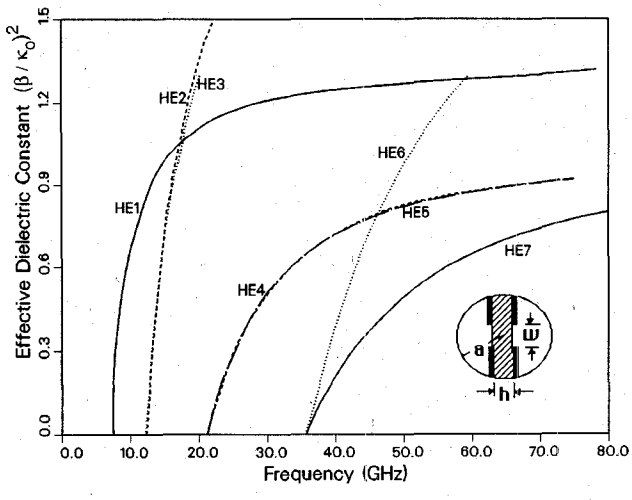

Fig. 4. Dispersion characteristics of a bilateral finline in circular waveguide housing (WC33). $a = 4.165$ mm, $h = 0.254$ mm, $w = 0.3$ mm, $\epsilon_r = 2.2$. ———— magnetic wall at $x = a/2$, electric wall at $y = b/2$; ---- electric wall at $x = a/2$, magnetic wall at $y = b/2$; · · · · · electric wall at $x = a/2$, electric wall at $y = b/2$; — · — magnetic wall at $x = a/2$, magnetic wall at $y = b/2$.

B. *Effect of Substrate Bending*

Bending of the substrate can occur when soft materials are used (mounting grooves too narrow result in displacement of dielectric material, producing bending). The propagation characteristics computed with bent substrate for deflections d of 0.125 mm and 0.25 mm are compared with those of the straight substrate in Fig. 3. It is found that the change in the propagation constant is negligible near cutoff and is slightly higher in the operating frequency band of the waveguide enclosure. This is attributed to the increased volume of dielectric material (due to bending) in the structure and the progressive confinement of energy in the dielectric as frequency increases.

C. *Bilateral Finlines in Circular Waveguide Housing*

It is interesting to note that an ultra-bandwidth finline coupler in circular waveguide housing was reported as

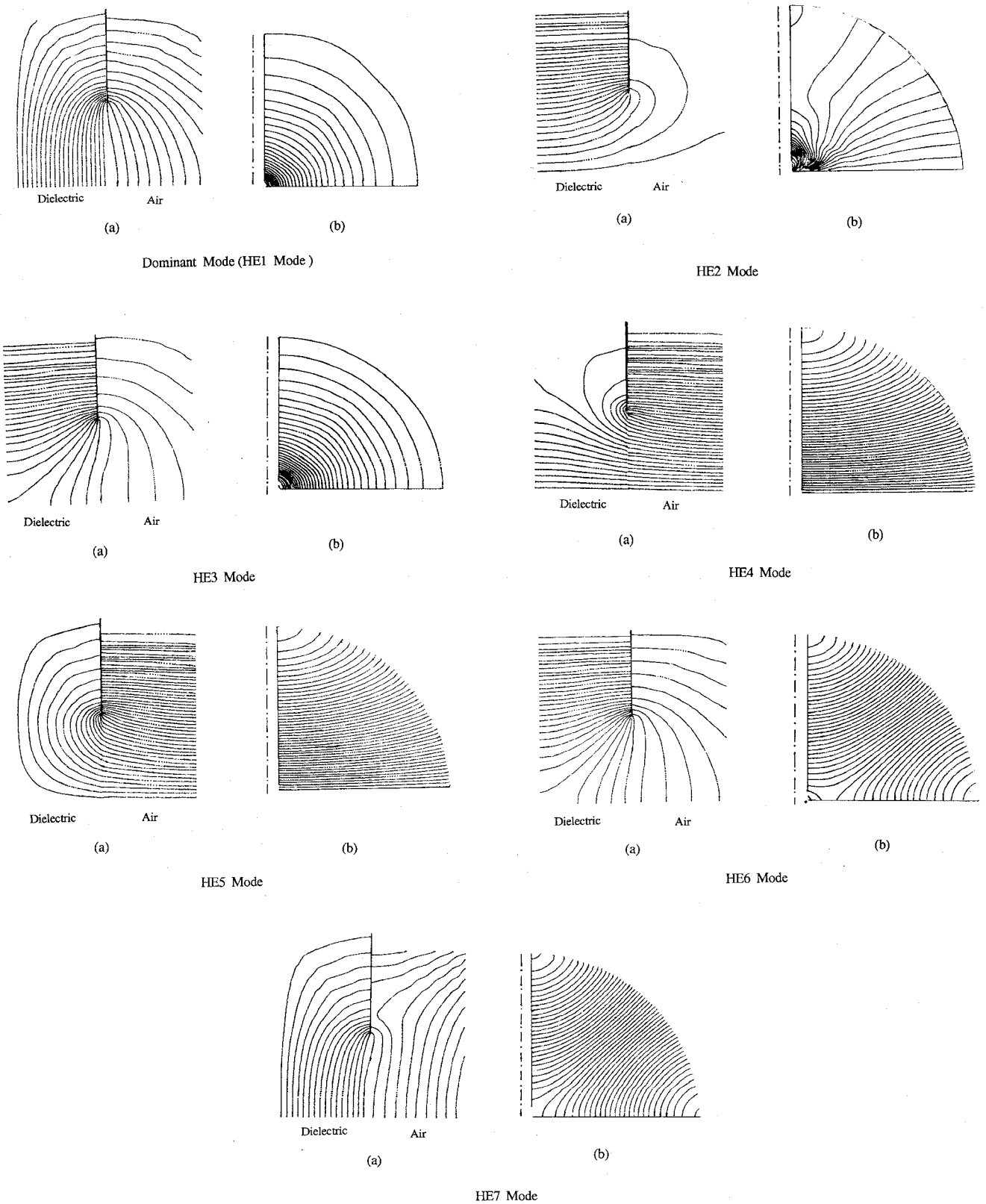

Fig. 5. Electric field lines of the dominant and higher order modes at cutoff in a bilateral finline in circular waveguide housing (WC33). $a = 4.165$ mm, $h = 0.254$ mm, $w = 0.3$ mm, $\epsilon_r = 2.2$. (a) Field in the slot region. (b) Field in the air region (only one quarter of cross section shown.

early as 1955 [15]. No theoretical analysis of such a structure has ever been published, probably due to the complexity of the problem. The advantages of such structures are easy fabrication and compatibility of the dominant mode with the TE_{11} mode of the circular waveguide.

The dispersion characteristics for the fundamental mode and six higher order modes are given in Fig. 4. All the results are obtained by analyzing only one quarter of the structure with four combinations of electric and magnetic walls. The HE_1 and HE_7 modes (solid lines), which are excited by a TE_{11} wave incident on the empty circular waveguide, will define the actually relevant monomode range. The electric field plots for the various modes are shown in Fig. 5. A thorough study of dispersion characteristics (over a wide range of finline parameters) and loss characteristics is in progress.

VI. Conclusion

In this paper, a finite element procedure for the analysis of generalized finlines is presented. The method is capable of handling shielded microwave and millimeter-wave transmission lines with arbitrary cross-sectional geometries. The method can also include finite metallization thickness, substrate mounting grooves, bending of the substrate, and even the cross-sectional profile of the metallization edges.

Results obtained for the dispersion characteristics for bilateral finlines in rectangular waveguide enclosure agree to within less than 1 percent with data computed by Schmidt [1] using the spectral-domain technique. Bending of the substrate causes a slight increase in the propagation constant of the dominant finline mode.

For the first time, the dispersion characteristics of bilateral finlines in circular waveguide enclosures are presented. Further studies are being conducted to compare such characteristics as monomode bandwidth, attenuation constant, and impedance range to those of the finlines in rectangular waveguide enclosure.

It may be noted that the finite element algorithm requires one to two orders of magnitude more CPU time and memory than a spectral-domain program for an idealized planar structure in a rectangular enclosure. However, the finite element approach develops its full potential when second-order effects and irregular geometries must be evaluated, a task at which most other numerical techniques fail.

References

[1] L. P. Schmidt and T. Itoh, "Spectral domain analysis of dominant and higher modes in finlines," *IEEE Trans. Microwave Theory Tech.*, vol. MTT-28, pp. 981–985, Sept. 1980.

[2] W. J. R. Hoefer and A. Ros, "Finline parameters calculated with the TLM-method," presented at 1979 IEEE MTT-S Int. Microwave Symp., Orlando, FL, Apr. 28–May 2, 1979.

[3] R. Vahldieck, "Accurate hybrid-mode analysis of various finline configurations including multilayered dielectrics, finite metallization thickness, and substrate holding grooves," *IEEE Trans. Microwave Theory Tech.*, vol. MTT-32, pp. 1454–1460, Nov. 1984.

[4] T. Kitazawa and R. Mittra, "Analysis of finline with finite thickness," *IEEE Trans. Microwave Theory Tech.*, vol. MTT-32, pp. 1484–1487, Nov. 1984.

[5] J. Bornemann and F. Arndt, "Calculating the characteristic impedance of finlines by transverse resonance method," *IEEE Trans. Microwave Theory Tech.*, vol. MTT-21, pp. 85–92, Jan. 1986.

[6] D. Mirshekar-Syahkal and J. B. Davies, "An accurate unified solution to various finline structures, of phase constant, characteristic impedance, and attenuation," *IEEE Trans. Microwave Theory Tech.*, vol. MTT-30, pp. 1854–1861, Nov. 1982.

[7] C. Olley and T. Rozzi, "Currents and conduction losses in unilateral finline," *IEEE Trans. Microwave Theory Tech.*, vol. 36, pp. 86–95, Jan. 1988.

[8] C. Yeh, K. Ha, S. B. Dong, and W. P. Brown, "Single-mode optical waveguides," *Appl. Opt.*, vol. 18, pp. 1490–1504, May 1979.

[9] M. Hano, "Finite element analysis of dielectric loaded waveguides," *IEEE Trans. Microwave Theory Tech.*, vol. MTT-32, pp. 1275–1279, Oct. 1984.

[10] A. Konrad, "High-order triangular finite elements for electromagnetic waves in anisotropic media," *IEEE Trans. Microwave Theory Tech.*, vol. MTT-25, pp. 353–360, May 1977.

[11] M. Koshiba, K. Hayata, and M. Suzuki, "Improved finite element formulation in terms of the magnetic field vector for dielectric waveguides," *IEEE Trans. Microwave Theory Tech.*, vol. MTT-33, pp. 227–233, Mar. 1985.

[12] T. Angkaew *et al.*, "Finite element analysis of waveguide modes: A novel approach that eliminates spurious modes," *IEEE Trans. Microwave Theory Tech.*, vol. MTT-35, pp. 117–123, Feb. 1987.

[13] P. Silvester, "High-order polynomial triangular finite elements for potential problems," *Int. J. Eng. Sci.*, vol. 7, pp. 849–861, 1969.

[14] P. Daly, "Finite element coupling matrices," *Electron. Lett.*, vol. 5, pp. 613–615, Nov. 27, 1969.

[15] S. D. Robertson, "The ultra-bandwidth finline coupler," *Proc. IRE.*, vol. 43, no. 6, pp. 739–741, June 1955.

[16] R. N. Bates and M. D. Coleman, "Finline for microwave integrated circuits (MICs) at *Ka*-band (27–40 GHz)," presented at IEE Colloq. Microwave Integrated Circuits Design, no. 1978/26, Apr. 1978.

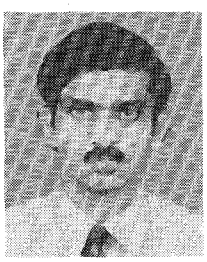

Eswarappa received the B.E. degree in electronics and communication from Mysore University, India, in 1980 and the M.Tech degree in electrical engineering from the Indian Institute of Technology, Kanpur, in 1982.

From 1982 to 1986, he worked as an Assistant Executive Engineer in the Transmission Research and Development Laboratory, Indian Telephone Industries, Bangalore, India. He was mainly engaged in the design and development of microwave circuits and the characterization of microstrip discontinuities. Since 1986 he has been engaged in research on quasi-planar transmission media and numerical techniques, and he is working toward the Ph.D degree in electrical engineering at the University of Ottawa, Ottawa, Ont., Canada.

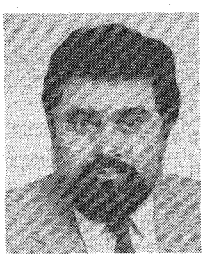

George I. Costache (M'78–SM'82) is an Associate Professor and Chairman of the Electrical Engineering Department at the University of Ottawa, Ottawa, Ont., Canada. His career has included positions with the University of Manitoba, the University of Manchester, and Electricité de France. He has taught electromagnetics and numerical techniques applied to electromagnetics for more than 18 years and has made original contributions to the solution of skin-effect problems and electromagnetic transient

phenomena. His main interest is in numerical techniques, such as finite-element analysis and moment methods, and their application to interference problems in steady-state and time-domain applications.

The author or coauthor of over 50 technical papers and reports, Dr. Costache is a member of the editorial review board of *COMPEL*, the international journal for computation and mathematics in electrical and electronics engineering. He is a registered Professional Engineer in the province of Ontario, Canada.

✠

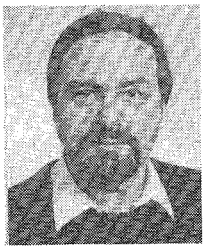

Wolfgang J. R. Hoefer (M'71–SM'78) received the diploma in electrical engineering from the Technische Hochschule Aachen, Aachen, Germany, in 1964 and the D. Ing. degree from the University of Grenoble, Grenoble, France, in 1968.

After one year of teaching and research at the Institut Universitaire de Technologie, Grenoble, France, he joined the Department of Electrical Engineering, University of Ottawa, Ottawa, Ont., Canada, where he is currently a Professor. His sabbatical activities have included six months with the Space Division of the AEG-Telefunken in Backnang, Germany, six months with the Electromagnetics Laboratory of the Institut National Polytechnique de Grenoble, France, and one year with the Space Electronics Directorate of the Communications Research Centre in Ottawa, Canada. His research interests include microwave measurement techniques, millimeter-wave circuit design, and numerical techniques for solving electromagnetic problems.

Dr. Hoefer is a registered Professional Engineer in the province of Ontario, Canada.